

Evolution of microstructure and impact-strength energy in thermally and thermomechanically aged 15-5 PH

Emilie Herny, Philippe Lours, Eric Andrieu, Jean-Marc Cloué, Philippe Lagain

▶ **To cite this version:**

Emilie Herny, Philippe Lours, Eric Andrieu, Jean-Marc Cloué, Philippe Lagain. Evolution of microstructure and impact-strength energy in thermally and thermomechanically aged 15-5 PH. Proceedings of the Institution of Mechanical Engineers, Part L: Journal of Materials: Design and Applications, 2008, vol. 222 (n° 4), pp.299-304. hal-01688569

HAL Id: hal-01688569
https://hal.science/hal-01688569

Submitted on 4 Dec 2019

HAL is a multi-disciplinary open access archive for the deposit and dissemination of scientific research documents, whether they are published or not. The documents may come from teaching and research institutions in France or abroad, or from public or private research centers.

L'archive ouverte pluridisciplinaire **HAL**, est destinée au dépôt et à la diffusion de documents scientifiques de niveau recherche, publiés ou non, émanant des établissements d'enseignement et de recherche français ou étrangers, des laboratoires publics ou privés.

Evolution of microstructure and impact-strength energy in thermally and thermomechanically aged 15-5 PH

E Herny[1,2], **P Lours** *[1], **E Andrieu**[2], **J M Cloué**[3], and **P Lagain**[4]
[1]CROMeP-Ecole des Mines d'Albi-Carmaux, Campus Jarlard Albi, France
[2]CIRIMAT-ENSIACET, Laboratoire du CIRIMAT UMR5085 CNRS, Toulouse, France
[3]Areva NP, Lyon, France
[4]Airbus France, site de St Martin, Toulouse, France

Abstract: Due to its outstanding mechanical resistance and resistance to corrosion, alloy 15-5 PH can be beneficially used for manufacturing aerospace structural parts. Following exposure to intermediate temperature, from 300°–400 °C, the alloy embrittles through the decomposition of the martensite into iron-rich and chromium-rich domains. Depending on the ageing time, these domains are either interconnected or unconnected with each other. The embrittlement results in a drastic drop of the impact strength-energy and an increase of the ductile-to-brittle transition temperature. The initial microstructure and mechanical properties can be recovered through a re-homogenization of the distribution of chromium and iron atoms in the material in the case where the decomposition of the matrix is not too pronounced. The application of a stress higher than 60 per cent of the yield strength further enhances the ageing kinetics in the case where the combined effect of temperature and time results in the spinodal decomposition of the martensite.

Keywords: PH steel, ductile-to-brittle transition, ageing, spinodal decomposition, martensite

1 INTRODUCTION

Structural applications in the aerospace industry require reliable, satisfactorily corrosion resistant, metallurgically stable metal alloys with high mechanical performance. Among various metal alloys, martensitic stainless steels, strengthened both by the diffusionless formation of soft martensite and the precipitation of coherent particles, have been used for a long time. For instance, for aerospace applications in the field of engine pylon manufacturing, alloy 15-5 PH is commonly used. In this industrial case, which is covered by the technical approach of the study, engine pylon parts are subject to specific mechanical loading, typically mechanical impact and shock coupled with long term thermal ageing. The metallurgical structure of such an alloy, on which this article focuses, is quite complex, and is the result of a long development process, aimed at improving the mechanical properties, ductility, and corrosion resistance of martensitic steels. Initially, steels rich in carbon and copper, and poor in nickel, and martensitic are hardened only by the main tempered martensite phase and showed low resistance to corrosion, because of the formation of chromium carbides resulting in Cr depleted zones, and low ductility, because of the formation of δ ferrite. At a more advanced stage of material development, the contents in carbon and nickel are respectively lowered and increased in order to limit the formation of such phases. Finally, copper is incorporated to promote the precipitation of strengthening particles finely dispersed in the martensite matrix. It is widely reported that such high chromium steels are sensitive to thermal ageing when exposed to temperatures close to 300 °C [**1**]. An increase of hardness and yield strength is generally observed, together with a significant loss of ductility and a dramatic increase of the ductile-to-brittle transition temperature (T_{DBT}) [**2**]. Many previous works suggested that the material ageing in the temperature range 300–400 °C and the correlated degradation of the mechanical properties

*Corresponding author: CROMeP-Ecole des Mines d'Albi-Carmaux, Campus Jarlard Albi Cedex 09, 81013, France. email: lours@enstimac.fr

are mainly due to the demixtion of the martensite into an iron-rich and a chromium-rich phase. Demixtion can either proceed through a diffusion driven nucleation and growth precipitation process or through the spinodal decomposition of the martensite. The level of embrittlement as well as the ageing kinetics depended not only on the exposure temperature and time, but also on the level of stress applied during ageing [**3**]. The aim of the study is to address the influence of ageing conditions on the ductile-to-brittle transition in alloy 15-5 PH, and to discuss its evolution in terms of metallurgical and microstructural changes. In order to investigate the influence of the ageing temperature, the ageing time and a concomitant applied stress, specimens for impact strength energy measurements, either free of stress or a under four-point bending load, are exposed at 350 and 400 °C for periods ranging from 15 h to 5000 h. Additional hardness measurements, tensile tests and microstructural analyses are used to complete the investigation.

2 EXPERIMENTAL

Martensitic stainless steel 15-5 PH, manufactured by Aubert and Duval using argon oxygen degassing (AOD) plus electro-slag remelting (ESR) techniques and cross-rolling down to 15 mm thick plate, corresponds to the ARMCO PH 15-5, namely AFNOR X5CrNiCu15-5. Its chemical composition is given in Table 1. The overall hardening thermal treatment of the alloy consists of: (a) solutionizing at 1050 °C for 30 min, (b) air quenching, and (c) tempering at 550 °C for 4 h at a heating rate of 2.5 °C/min.

Conventional impact strength energy measurements are carried out using an instrumented Amsler (300 J) pendulum. The investigated specimens are 55 mm long with nominal cross-sections of $6 \times 10\,mm^2$, and have lateral notches with depths of 0.5 mm and radii of curvature of 0.25 mm. This specific geometry allows the confinement of the fracture path and reduces the dispersion of the experimental results. It is adopted for all specimens in order to get the clear and unambiguous possibility of comparing results obtained in thoroughly controlled experimental conditions [**4**]. Tensile tests are performed at room temperature on aged specimens with a cross-section of $3 \times 1\,mm^2$, using an MTS (materials test system) electromechanical machine with a load cell of 5000 N and a strain rate of $10^{-3}\,s^{-1}$. Hardness values are determined by microhardness (under 300 g) and Vickers hardness Hv 30. Microstructural analysis is conducted using various techniques such as scanning electron microscopy (SEM), transmission electron microscopy (TEM), energy dispersive spectroscopy (EDS), and tomographic atom probe for the fine investigation of the volume distribution of individual atoms in the material.

3 RESULTS AND DISCUSSION

3.1 Microstructure

Figures 1 and 2 are two TEM micrographs showing the microstructure of alloy 15-5 PH. Tempering promotes

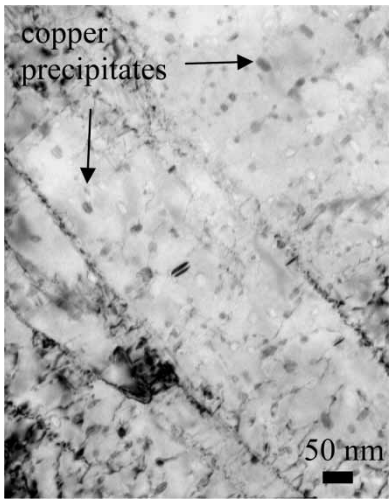


Fig. 1 TEM micrograph showing the fine precipitation of copper particles

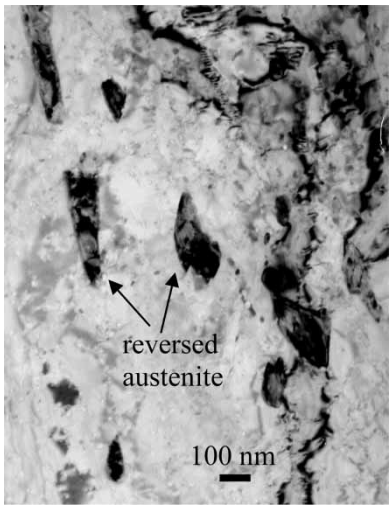


Fig. 2 TEM micrograph showing reversed austenite

Table 1 Composition of 15-5 PH (wt%)

C	Si	Mn	S	P	Ni	Cr	Mo	Cu	Nb	Ta	Fe
0.022	0.38	0.8	<0.002	0.015	4.91	14.83	0.25	3.02	0.19	<0.05	Balance

both the precipitation of coherent copper particles (Fig. 1) and the formation of reversed austenite (Fig. 2). The copper precipitates strengthen the material and the reversed austenite formed at former austenite grain boundaries softens the material. As a consequence, the co-existence of these two phases within the martensitic matrix ensures the required compromise among strength, ductility, and toughness.

3.2 Ageing with no stress

Plots of the impact strength energy measured at various temperatures from 100–500 °C as a function of the exposure time are given in Figs 3 and 4, respectively, for ageing temperatures of 350 and 400 °C. the ductile-to-brittle transition curve for the reference non-aged material is included in the figure.

For the two ageing temperatures, the ductile-to-brittle transition curves tend to flatten and shift towards the high temperatures as the ageing time increases. This results in a decrease of the impact strength energy characteristics of the ductile plateau and an increase of the ductile-to-brittle transition temperature. This overall embrittlement and the sensitivity to ageing are further enhanced when ageing time is increased. However, at exposure as early as 100 h, material properties show a significant evolution leading to a 25 and a 40 °C increase in T_{DBT}, respectively, for ageing at 350 and 400 °C. Of course, the ageing effects are even more pronounced if the ageing time is longer. For 1000 h ageing, the ductile-to-brittle transition temperature T_{DBT} is 86 and 177 °C, respectively higher than that of the reference material, for ageing at 350 and 400 °C. In this case (1000 h), the impact strength energy of the ductile plateau is about 50 per cent lower than that of the reference material, for both ageing temperatures.

Note that after 5000 h exposure at 350 and 400 °C, an additional transition is observed starting with test temperatures higher than 450 °C. At these temperatures, the material roughly recovers the impact strength energy of the unaged material, indicating a simple heat treatment at this temperature, which allows regeneration of the mechanical properties of the material, and thus, its microstructure.

The tensile curves obtained after ageing for 5000 h at 350 and 400 °C are compared with the tensile plot of the initial non-aged material in Fig. 5. Note that in each case, almost no strain hardening is measured. The yield strength is higher and the elongation to rupture is lower for the aged materials. A slight difference between the two aged alloys is observed. Though the yield strength is slightly higher for the specimen aged at 400 °C, its elongation to fracture remains surprisingly higher. This is attributed to the possible precipitation of complementary reversed austenite during long-term ageing. Indeed, the formation of this phase is supposed to be particularly enhanced at

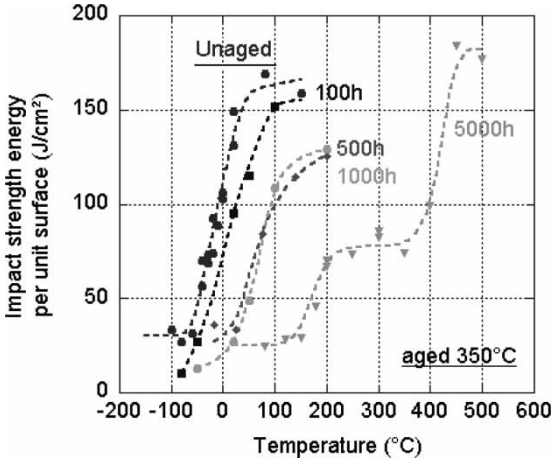


Fig. 3 Ductile to brittle transition for alloy 15-5 PH, unaged and aged at 350 °C

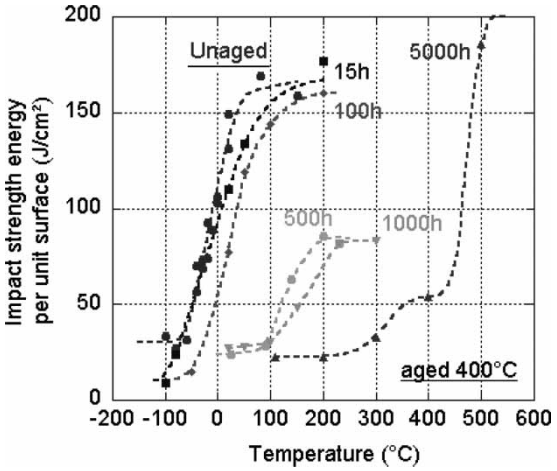


Fig. 4 Ductile to brittle transition for alloy 15-5 PH, unaged and aged at 400 °C

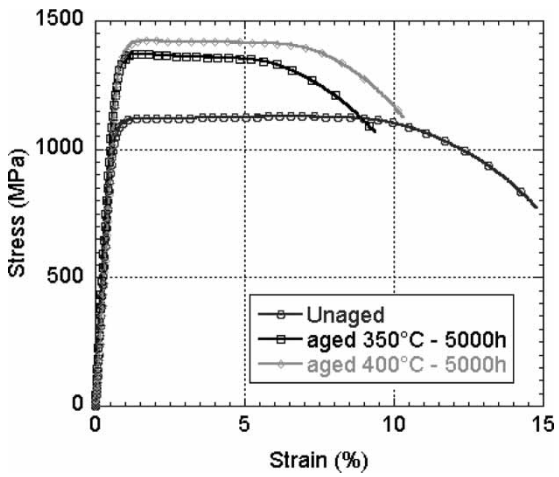


Fig. 5 Stress–strain curves for 15-5 PH, unaged and aged 5000 h at 350 and 400 °C

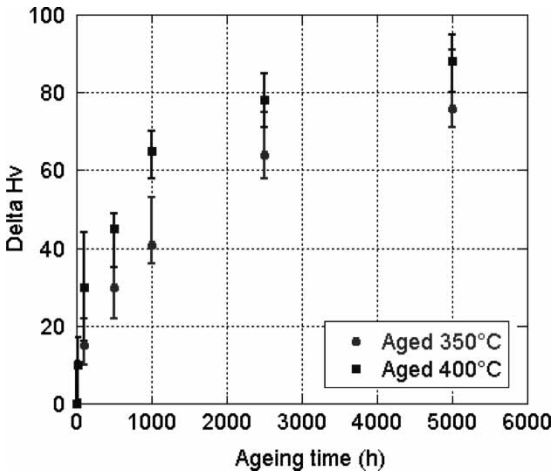


Fig. 6 Difference ΔHv in Vickers hardness between unaged alloy and alloy aged at 350 and 400 °C

temperatures close to 400 °C. The consequent increase in the volume fraction of reversed austenite could also explain the progressive softening observed elsewhere for a given ageing temperature as the exposure time increases [**5**]. Note that this softening, however, does not show the impact strength energy curves. This is due to the instability of the reversed austenite, which is prone to transform into martensite when loaded at high strain-rate during impact tests.

Correlatively to the increase in flow stress, the Vickers hardness of the material increases with the ageing time and ageing temperature. Figure 6 shows the hardness increment of specimens aged under various conditions with respect to the value of the unaged material. The hardness continually increases with ageing time and tends to level off for ageing times between 2500 and 5000 h.

A model proposed in reference [**2**] for a steel similar to 15-5 PH, and based upon microstructural and compositionnal considerations only, predicts a maximum increase of 130 HV for long term exposure at 400 °C. This value is slighly higher than the value measured for 15-5 PH aged for 5000 h, suggesting that the microstructural evolution leading to the change in hardness is still not completed within this exposure time.

3.3 Microstructure of the aged alloys

Basically, four types of metallugical transformations have been observed in the material after ageing. The first three are essentially investigated using TEM. They are: (a) the precipitation of chromium carbides, $Cr_{23}C_6$, within the martensite inter-laths; (b) the supplementary precipitation of copper particles; and (c) the supplementary formation of reversed austenite. However, though important, they cannot fully explain the drastic change in mechanical properties described in the previous section [**3**]. As a consequence they are not discussed in the following. The existence of a miscibilty gap in the iron-chromium equilibrium diagram [**6**] is much more likely to justify the evolution of the ductile-to-brittle transition and the correlated microstructural changes. The miscibilty gap may provoke the demixtion of the martensite matrix, provided the material is exposed at a given temperature, within the gap, for a given time. As indicated in section 1, demixtion can either proceed through the precipitation of the brittle α' phase or through the spinodal decomposition of the martensite, e.g. the fluctuations in composition resulting from the spinodal decomposition are prevalent on a microstructural scale much too fine to be easily resolved using TEM. The tomographic atom probe has been used to discriminate the various metallurgical states following various ageing parameters. The technique allows imaging of the distribution of atoms, in an elementary volume of material, with typical dimensions $6 \times 6 \times 40\,nm^3$ in our case.

Figure 7 shows the distribution of chromium atoms for a specimen aged for 1000 h at 400 °C. This distribution is obviously not homogeneous. As a consequence, an inter-connected network of chromium-enriched domains is observed. An additional analysis of iron atoms has revealed the same type of interconnected networks with iron-rich domains located in the chromium-depleted region. This fluctuation in the chemical composition, giving rise to alternate Cr-rich and Fe-rich domains, is typical of spinodal decomposition.

In Fig. 8, the morphology of the network is different, corresponding to the chromium distribution of a specimen aged for 5000 h at 400 °C. In this case, ageing being more pronounced, the chromium-rich domains are much more unconnected. This results in a depercolation of the network. In the former case, regenerating the alloy using a simple heat treatment was very difficult. For aging at higher temperatures, e.g. at 450 °C, the literature reports the precipitation of

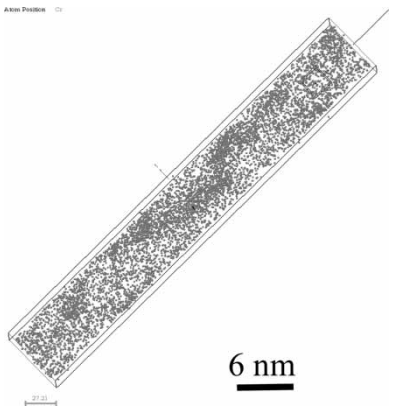


Fig. 7 Distribution of Cr atoms in alloy aged 1000 h at 400 °C (atomic probe)

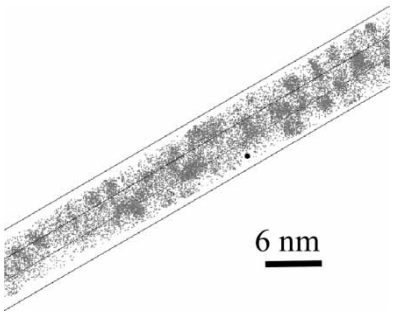


Fig. 8 Distribution of Cr atoms in alloy aged 5000 h at 400 °C (atomic probe)

α' [**7**] suggesting that the ageing mechanism changes between 400 and 450 °C.

3.4 Ageing under stress

The application of a stress during thermal exposure is performed using a specific, specially developed four-point bending equipment capable of embarking five Charpy specimens in a furnace. Finite element calculation was used to estimate the force required to load specimens with a stress higher than 80 per cent of the yield strength over a depth of 300 μm (about 10 metallurgical grains) at the tip of the Charpy notch. Additional ageing under stress is conducted on tensile specimens with multiple sections resulting, for a given applied uniaxial tension, in a multiple loading corresponding to various fractions of the yield strength. Figure 9 shows the ductile-to-brittle transitions curves of 15-5 PH aged for 1000 h at 350 and 400 °C under an applied four-points bending stress (full line). As a comparison, the transition plots of both the unaged material and of the material aged with no stress are given (dotted line). Note that the application of a stress does not result in any significant modification of the ductile-to-brittle transition curves. However, the role of an applied stress in accelerating the ageing kinetics has been proved in alloy PH13–8Mo, an alloy quite similar to 15-5 PH [**3**]. As a consequence, it is assumed that in the present case, the volume of material loaded during thermal exposure is not extended enough as compared with the volume of material taken into account for the calculation of the impact strength energy per unit surface. A thorough examination of the fracture surfaces of the specimens, either subjected or not, to an applied stress during exposure at high temperature, confirms this assumption when no morphological difference is observed.

Figure 10 compares the increment in Vickers hardness of specimens aged under tensile loading with the hardness of the reference unaged material. Tensile ageing is performed at 400 and 450 °C for 500 h, and hardness measurement is carried out in zones discontinuously loaded from 37 to 80 per cent of the yield strength. Whatever may be the level of the applied tensile stress at 450 °C, the hardness of the aged specimens is constant, 20 HV higher than the hardness of the unaged reference material. In this case, the thermal activation is high enough to provoke the precipitation of the α' phase; the formation of such a phase being further enhanced by the application of the stress.

At 400 °C, where ageing proceeds through the pinodal decomposition of the martensite, a rather high level of stress is necessary to provoke a significant increment in hardness. For example, the stress must be higher than roughly 60 per cent of the yield stress. For 80 per cent of the yield stress, the increase in hardness is about 20 HV.

The distribution of chromium atoms revealed by the atom probe microanalysis shows very similar features for the two types of specimens – either aged under

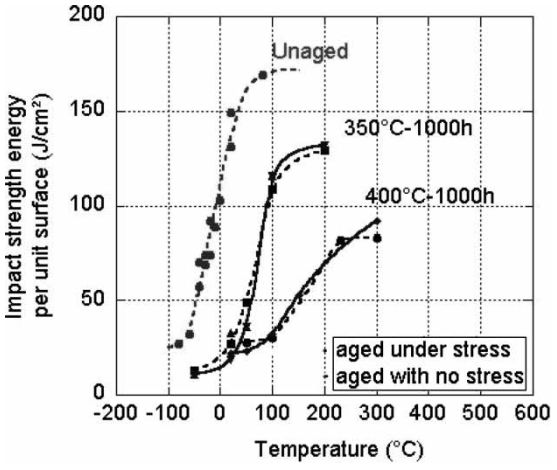


Fig. 9 Ductile to brittle transition for alloy 15-5 PH, unaged and aged under stress 1000 h at 350 and 400 °C

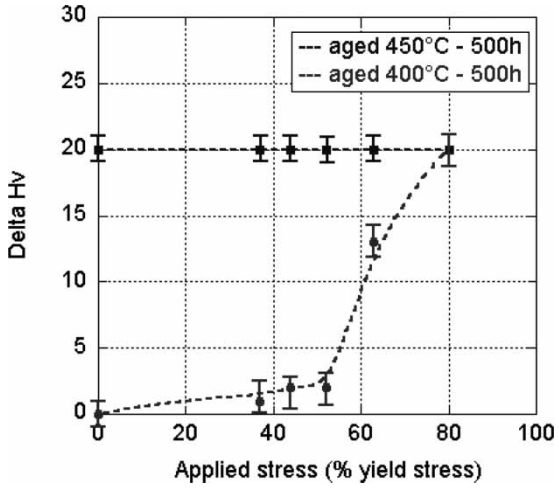


Fig. 10 Difference ΔHv in Vickers hardness between unaged alloy and alloy aged under stress at 400 and 450 °C

stress, or with no stress. However, a thorough analysis, showing a high differential between the theoretical and the experimental frequency distributions of chromium concentrations, indicated by the so-called V parameter [**8**, **9**], greatly suggests that the spinodal decomposition is enhanced when a stress is applied concomitantly to the temperature exposure. Such a V parameter for the material aged under stress for 500 h at 400 °C, is equivalent to that for the material aged for 1000 h with no stress, indicating a similar advancement of the spinodal decomposition in both cases. This former result is supported by the comparative measurement of hardness, reaching 430 HV in the two cases.

It is stated in references [**10**] and [**11**] that the volume distortion induced by the hydrostatic component of the applied stress tensor modifies the solubility of the chemical elements that can influence the initiation of the spinodal decomposition. Indeed, when the process of spinodal decomposition has been initiated, the hydrostatic component of the stress tensor is much lower than the stress generated by the demixtion itself, so that it is no longer operative in accelerating the metallurgical change responsible for the evolution of the mechanical properties. Thermomechanical ageing under pure shearing, that is, with a hydrostatic stress component equal to zero, results in the same hardness increment as ageing under uniaxial tension [**5**]. As a consequence, it is concluded that hydrostatic stress has no influence on ageing kinetics. Though hydrostatic stress is operative in initiating spinodal decomposition, it is only deviatoric stress that is reponsible for the development of the transformation.

4 CONCLUSION

Ageing the alloy 15-5 PH at temperatures of 350 and 400 °C results in a significant drop of the impact strength energy, and a shift of the ductile-to-brittle transition temperature towards a higher level. In addition, both the yield strength and the hardness of the material increase upon exposure to temperature. It is shown that the evolution of those mechanical properties is related to a metallurgical transformation of the martensite, the major phase of the material. This transformation proceeds through the demixtion of the martensite, resulting in the formation of alternate Cr and Fe rich domains through the spinodal decomposition. At 450 °C, above the miscibility gap shown in the Fe–Cr equilibrium diagram, the demixtion results from the precipitation of the Cr rich α' phase, which also embrittles and hardens the material. The application of a stress higher than 60 per cent of the yield strength together with the exposure to temperature accelerates the ageing kinetics. It is shown that only the deviatoric component of the stress is responsible for the enhancement of the ageing kinetics. The embrittlement is reversible, provided an appropriate heat treatment is performed on the aged alloy. However, this regeneration treatment is only effective if the interconnected network formed during ageing has not reached its depercolation limit.

ACKNOWLEDGEMENTS

Authors gratefully acknowledge F. Danoix, Université de Rouen, France, for performing Atome Probe Analysis and for providing fruitfull advices and discussion on the interpretation of data.

REFERENCES

1 **Guo, Z., Sha, W.,** and **Vaumousse, D.** Microstructural evolution in a PH13-8 stainless steel after ageing. *Acta Materialia*, 2003, **51**, 101–116.

2 **Delarboulas, M.** and **Cozar, R.** Caractéristiques et Possibilités d'Applications Aérospatiales de l'Acier E Z3 CNDA 13-08. *Matériaux et Techniques*, 1985, **10–11**, 619–631.

3 **Eberle, A., Klingbeil, D., Baer, W., Wossidlo, P.,** and **Häcker, R**. The calculation of dynamic J_R curves from 2D and 3D finite element analysis of Charpy tests using a rate dependent damage model. In Proceedings of the *From Charpy to Present Impact Testing* Conference (Eds D. François and A. Pineau), 2002, pp. 403–410 (ESYS Publication, Paris).

4 **Cloue, J. M.** *Justification de la Tenue en Service en Milieu Primaire REP d'un Acier Martensitique à Durcissement Structural*. PhD Thesis, Ecole des Mines de Paris, 1998.

5 **Herny, E.** *Caractérisation mécanique et étude des mécanismes de vieillissement thermique et thermomécanique de l'acier inoxydable martensitique 15-5PH, soudé par faisceau d'électrons*. PhD Thesis, Institut National Polyechnique de Toulouse, 2006.

6 **Leslie, W. C.** *The physical metallurgy of steel*, 1981 (TechBooks, Hemisphere Publishing Corporation).

7 **Vrinat, M., Cozar, R.,** and **Meyzaud, Y.** Precipitated phases in the ferrite of aged cast duplex stainless steels. *Scripta Materialia*, 1986, **20**, 1101–1106.

8 **Danoix, F.** *Phénomène de Décomposition de la Ferrite des Aciers Austéno-ferritiques. Une Etude par Microscopie Ionique et Microanalyse à la Sonde Atomique*. PhD Thesis, Université de Rouen, 1991.

9 **Danoix, F.** and **Auger, P.** Atom robe studies of the Fe-Cr system and stainless steels Aged at intermediate temperature: a review. *Mater. Character.*, 2000, **44**, 177–201.

10 **Larché, F. C.** What can the concept of a perfect chemoelastic solid tell us about the mechanical and thermodynamic behaviour of a solid. *Journal de Physique IV, Colloque C1*, 1996, **6**, 3–9.

11 **Larché, F. C.** and **Cahn, J. W.** The interactions of composition and stress in crystalline solids. *Acta Materialia*, 1985, **33**(85), 331–357.